

## ARTICLE TYPE

# Fixed-time Integral Sliding Mode Control for Admittance Control of a Robot Manipulator

Yuzhu Sun<sup>1</sup> | Mien Van<sup>\*2</sup> | Stephen McIlvanna<sup>3</sup> | Seán McLoone<sup>4</sup> | Dariusz Ceglarek<sup>5</sup>

<sup>1</sup>School of electronics, electrical and computer science, Queen's University of Belfast, Belfast, UK

<sup>2</sup>School of electronics, electrical and computer science, Queen's University of Belfast, Belfast, UK

<sup>3</sup>School of electronics, electrical and computer science, Queen's University of Belfast, Belfast, UK

<sup>4</sup>School of electronics, electrical and computer science, Queen's University of Belfast, Belfast, UK

<sup>5</sup>Warwick Manufacturing Group, University of Warwick, Coventry, UK

**Correspondence**

\*Mien Van, School of electronics, electrical and computer science, Queen's University of Belfast, Belfast BT7 1NN. Email: M.Van@qub.ac.uk

**Summary**

This paper proposes a novel fixed-time integral sliding mode controller for admittance control to enhance physical human-robot collaboration. The proposed method combines the benefits of compliance to external forces of admittance control and high robustness to uncertainties of integral sliding mode control (ISMC), such that the system can collaborate with a human partner in an uncertain environment effectively. Firstly, a fixed-time sliding surface is applied in the ISMC to make the tracking error of the system converge within a fixed-time regardless of the initial condition. Then, a fixed-time backstepping controller (BSP) is integrated into the ISMC as the nominal controller to realize global fixed-time convergence. Furthermore, to overcome the singularity problem, a non-singular fixed-time sliding surface is designed and integrated into the controller, which is useful for practical application. Finally, the proposed controller is validated for a two-link robot manipulator with uncertainties and external human forces. The results show that the proposed controller is superior in the sense of both tracking error and convergence time, and at the same time, can comply with human motion in a shared workspace.

**KEYWORDS:**

Integral sliding mode control, fixed-time convergence, admittance control, robot manipulator, physical human-robot collaboration

## 1 | INTRODUCTION

Recent developments in the biomedical, social and industrial robotics have led to an increasing interest in the field of physical human-robot collaboration (pHRC).<sup>1,2</sup> Robots that can physically collaborate with human partners enable the cognitive strengths of human and the high-precision and repeatability of robots to be combined. Unlike fully automated industrial production lines, to effectively work with the human partner in a shared workspace involving activities such as object handovers or co-carrying, it is imperative that the cooperative robots are capable of simultaneously complying with human forces at the contact point rather than rejecting them as external disturbances.<sup>3</sup> Therefore, impedance/admittance control based compliance control strategies have been attracting significant interest for this application. These include the adaptive admittance control,<sup>4</sup> adaptive impedance control,<sup>5,6</sup> and robust impedance control.<sup>7,8</sup>

Consider an industrial robot that is required to work with a human partner in an uncertain environment. The controller of the robot should be capable of tracking a certain trajectory with external uncertainties and perturbations, and at the same time, be compliant to human forces without the loss of stability. A considerable literature exists on techniques for improving the tracking performance of robot manipulators in an uncertain environment. For many years, model-free control strategies such as PID have

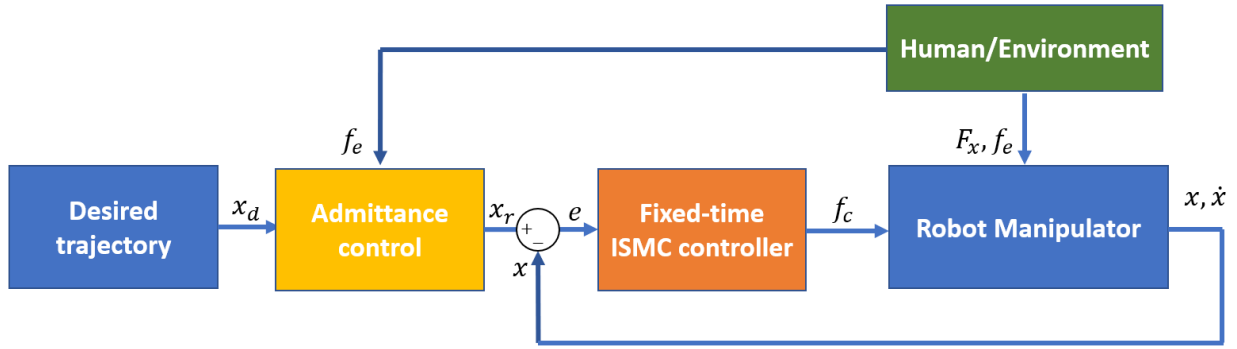


**FIGURE 1** Structure of the proposed FTISMCM Admittance Control Scheme.

been extensively employed in the industry.<sup>9</sup> Sliding mode control (SMC) based methods have also emerged and been widely studied in the field of robotics to provide robustness against the effects of parametric uncertainties and external disturbances.<sup>10</sup> The SMC scheme involves (i) the reaching phase, in which the system converges from the initial state to the sliding surface, and (ii) the sliding phase, in which the system reaches the sliding surface and tries to stay on the equilibrium point. However, the effectiveness of SMC is limited by the reaching phase which is sensitive to disturbances. Therefore, to overcome the limitation of SMC, integral sliding mode control (ISMC) has been developed. ISMC eliminates the reaching phase by finding a suitable initial position to reject disturbances from the beginning, which is helpful for practical applications.<sup>10</sup>

Furthermore, to obtain the property of fast tracking-error convergence, a further extension of ISMC, called fixed-time integral sliding mode control (FTISMCM),<sup>11,12,13</sup> which incorporates the benefits of ISMC and fixed-time sliding mode control (FxTSMCM)<sup>14</sup> has been proposed. Compared with traditional finite-time control strategies,<sup>15,16</sup> the fixed-time controller does not depend on the initial condition of the system with the result that the convergence time can be determined a priori based on the design parameters.<sup>16</sup> In the work of Huang and Wang,<sup>11</sup> a FTISMCM is proposed that stabilizes a highly complex nonlinear system within a fixed time and effectively restrains the irregular and nonlinear vibrations of the system. In the work of Li et al.<sup>12</sup> a new integral high order sliding mode controller is proposed for high-order nonlinear systems with fixed-time convergence. In addition, the singularity problem always comes up in the sense of fixed-time stability when calculating the derivative of sliding variables. To address this issue a number of approaches have been developed to avoid or eliminate the singularity.<sup>17,18,9,19,20</sup> In the work of Feng et al.<sup>17</sup> a global non-singular terminal sliding mode controller is presented for second-order systems to overcome the singularity problem. In the work of Zuo,<sup>19</sup> a new sliding surface is proposed to circumvent the singularity problem. In the work of Van and Ceglarek,<sup>20</sup> a new fault-tolerant control scheme based on a nonsingular fixed-time sliding mode controller is proposed for robot manipulators, which guarantees a global fixed-time convergence.

So far there is little literature that combines admittance control and FTISMCM for physical human-robot collaboration. Motivated by the above discussion this paper proposes a new ISMC control scheme for admittance control of a robot manipulator, as depicted in Fig. 1. The stability and tracking error of the closed-loop system are converged within a fixed time. Furthermore, for practical application, a nonsingular fixed-time integral sliding mode controller is designed. The proposed method is then simulated on a two-link robot manipulator and compared with other state-of-the-art control strategies. The simulation results show that the proposed controller is superior in the sense of both tracking error and convergence time. The contributions and innovations of the proposed approach can be highlighted in a comparison with other approaches as follows:

1. Compared to conventional admittance control,<sup>2</sup> the proposed approach integrates an admittance with a FTISMCM to guarantee a fixed-time convergence, while compliant with external forces. Therefore, the proposed controller provides faster transient response, lower tracking errors and better disturbance rejection capacity.
2. Compared to the existing FTISMCM,<sup>11,12,13</sup> which uses the tracking errors and the velocity of the tracking errors to reconstruct the integral sliding surface, the proposed controller develops a new nonsingular fixed-time sliding surface and uses the dynamics model of the system, which is reconstructed based on the nonsingular fixed-time sliding surface, to reconstruct a new integral sliding surface. Therefore, the proposed approach is able to avail of the full advantages of both ISMC and FxTSMCM.

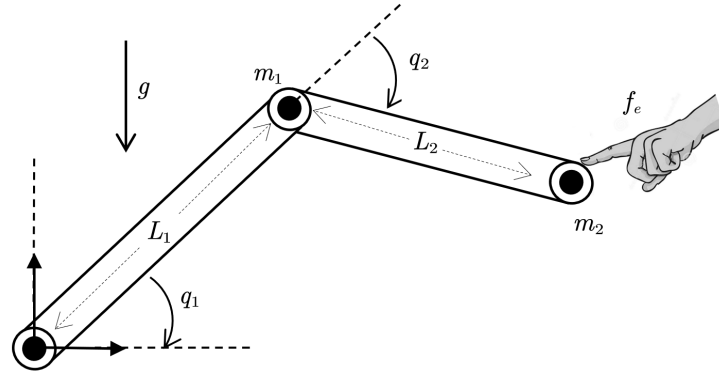


**FIGURE 2** Two-Link robot manipulator.

The paper is organized as follows. The mathematical model describing the motion of a robot manipulator and the problem formulation are presented in Section 2. The proposed fixed-time ISMC scheme for admittance control is developed in Section 3. Simulation results demonstrating the effectiveness of the proposed controller are presented in Section 4. Finally, section 5 discusses the conclusions and directions for future works.

## 2 | PROBLEM FORMULATION AND PRELIMINARIES

### 2.1 | Problem Formulation

We consider a robot manipulator whose joint space dynamics equation can be written in the form:

$$M(q)\ddot{q} + C(q, \dot{q})\dot{q} + G(q) + F(\dot{q}) = \tau_c + \tau_e \quad (1)$$

where  $q$ ,  $\dot{q}$ ,  $\ddot{q}$  are the joint positions, velocities and accelerations of the robot manipulator, respectively.  $q = [q_1, q_2, \dots, q_N]^T$  and  $N$  is the number of joints.  $M(q)$  is the  $N \times N$  mass matrix,  $C(q, \dot{q})$  is the  $N \times N$  Coriolis and centrifugal forces matrix,  $G(q)$  is the  $N \times 1$  gravity vector, and  $F(\dot{q})$  is the  $N \times 1$  vector of frictional forces.  $\tau_c$  denotes the control torque acting at the joints, and  $\tau_e$  is the external torque from the interaction with the human partner.  $F(\dot{q})$  and  $\tau_e$  together form the time-varying lumped uncertainties of the system. Fig. 2 above shows the structure of a classical two-link robot manipulator interacting physically with a human.

Since it is easier to formulate the trajectory in Cartesian space, we transfer the joint space dynamics of the robot manipulator (1) into Cartesian space:

$$M_x \ddot{x} + C_x \dot{x} + G_x + F_x = f_c + f_e \quad (2)$$

where  $x = [x_1, x_2, \dots, x_N]$  is the position of the joints in Cartesian space,  $M_x$ ,  $C_x$ ,  $G_x$  and  $F_x$  are coefficient matrices in Cartesian space,  $f_c$  is the control force, and  $f_e$  is the external force. The joint space velocities and Cartesian space velocities are related as:

$$\dot{x} = J(q)\dot{q} \quad (3)$$

where  $J(q)$  is the Jacobian of the robot manipulator. Inserting (3) into (1), the coefficient matrices in Cartesian space can be written as:

$$\begin{aligned} M_x &= J^{-T}(q) M(q) J^{-1}(q) \\ C_x &= J^{-T}(q) (C(q, \dot{q}) - M(q) J^{-1}(q) \dot{J}(q)) J^{-1}(q) \\ G_x &= J^{-T}(q) G(q), \quad F_x = J^{-T}(q) F(\dot{q}) \\ f_c &= J^{-T}(q) \tau_c, \quad f_e = J^{-T}(q) \tau_e \end{aligned}$$

Letting  $\eta_1 = x$  and  $\eta_2 = \dot{x}$ , the Cartesian space model of the robot can be represented as:

$$\begin{cases} \dot{\eta}_1 = \eta_2 \\ \dot{\eta}_2 = M_x^{-1} (-C_x \dot{x} - G_x - F_x + f_e + f_c) \end{cases} \quad (4)$$

For ease of control design, let  $\Xi = M_x^{-1}$ ,  $\Gamma(x, \dot{x}) = M_x^{-1}(-C_x - G_x)$ ,  $\Psi(x, \dot{x}, t) = M_x^{-1}(-F_x + f_e)$ , and  $u = f_c$ , such that the Cartesian space model can be further written as:

$$\begin{cases} \dot{\eta}_1 = \eta_2 \\ \dot{\eta}_2 = \Xi u + \Gamma(x, \dot{x}) + \Psi(x, \dot{x}, t) \end{cases} \quad (5)$$

**Assumption 1:** There exists a positive constants  $\rho$ , such that the unknown lumped uncertainties term is bounded by:

$$\Psi(x, \dot{x}, t) = M_x^{-1}(-F_x + f_e) \leq \rho \quad (6)$$

where  $\rho$  is a positive constant.  $\Psi(x, \dot{x}, t) = [\Psi_1(x, \dot{x}, t), \dots, \Psi_N(x, \dot{x}, t)]^T$ . This assumption means that the lumped uncertainties such as joint errors, friction and external human forces are bounded, which is usually satisfied in real application scenarios.

The control objective of this paper is to develop a fixed-time ISMC scheme to make the joint position  $x$  track a certain trajectory  $x_r$ , which is generated from admittance control. Therefore, the robot manipulator can comply with human forces rather than reject them as external disturbances. Furthermore, we require that the tracking error converges within an arbitrarily small interval of time, regardless of the initial conditions.

## 2.2 | Preliminaries

Consider a time-varying differential equation:

$$\dot{x} = f(x, t) \quad (7)$$

where  $x \in R^n$ , and  $f : R^n \rightarrow R^n$  is a continuous nonlinear function. Assume that the origin of (7) is the stable equilibrium point and  $f(0) = 0$ .

**Definition 1<sup>9</sup>:** The system (7) is finite time stable if the origin is Lyapunov stable and any solution  $x(t)$  starting from  $x_0$  satisfies  $\lim_{t \rightarrow T(x_0)} x(t) \rightarrow 0$  and  $x(t) = 0, \forall t > T(x_0)$ , where  $T(x_0)$  represents the settling time of the system.

**Definition 2<sup>9</sup>:** The system (7) is fixed-time stable if it is globally finite time stable and its settling time  $T(x_0)$  satisfies  $T(x_0) < T_{\max}$ , where  $T_{\max}$  is a positive number.

**Lemma 1<sup>16</sup>:** The following inequality holds for any real number that satisfies  $x_1, x_2, \dots, x_n > 0$  and  $0 < k < 1$ :

$$\sum_{i=1}^n x_i^{k+1} \geq \left( \sum_{i=1}^n x_i^2 \right)^{\frac{k+1}{2}} \quad (8)$$

**Lemma 2<sup>16</sup>:** The following inequality holds for any real number that satisfies  $x_1, x_2, \dots, x_n > 0$  and  $k > 1$ :

$$\sum_{i=1}^n x_i^k \geq n^{1-k} \left( \sum_{i=1}^n x_i \right)^k \quad (9)$$

**Lemma 3<sup>16</sup>:** Consider a scalar differential system below:

$$\dot{y} = \lambda_1 [y]^\alpha + \lambda_2 [y]^\beta, \quad y(0) = y_0 \quad (10)$$

where  $\lambda_1, \lambda_2, \alpha, \beta$  are all positive real number satisfying  $\lambda_1, \lambda_2 > 0$ ,  $0 < \alpha < 1$  and  $\beta > 1$ . Then the system (10) is fixed-time stable and the convergence time is independent with respect to the initial state of the system and upper bounded by the design parameters as:

$$T(x_0) < T_{\max} = \frac{1}{\lambda_1(1-\alpha)} + \frac{1}{\lambda_2(\beta-1)} \quad (11)$$

## 3 | CONTROL DESIGN AND STABILITY ANALYSIS

### 3.1 | Admittance Trajectory Shaping

To comply with external human forces, the system at the contact point can be modeled as a mass-spring-damper system (shown in Fig. 3). The objective of modeling the system with virtual mass, spring and damper is to make sure the interaction forces are elastic and never vibrate at the contact point.

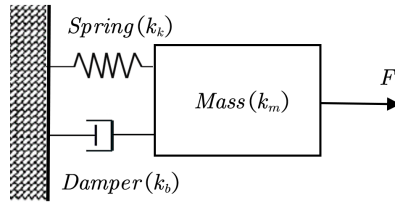


**FIGURE 3** The mass-spring-damper system.

Let  $\xi_i = x_{r_i} - x_{d_i}$ ,  $i = 1, 2, \dots, N$ , where the  $x_{r_i}$  is the reference trajectory generated from admittance control and the  $x_{d_i}$  is the initial desired trajectory of the robot manipulator. The dynamics for a robot manipulator rendering an impedance can be written as:

$$k_m \ddot{\xi}_i + k_b \dot{\xi}_i + k_k \xi_i = f_e \quad (12)$$

where  $k_m$ ,  $k_b$  and  $k_k$  are mass, spring and damping coefficient.  $f_e$  is the external human force. By integrating the impedance equation (12), we obtain  $x_{r_i}$  which will be tracked by the controller.

### 3.2 | Design of Fixed-time ISMC

Let the tracking error be written as:

$$e = x - x_r \quad (13)$$

where  $x_r$  is the reference trajectory generated from the admittance control, and  $x$  is the real trajectory of robot. The derivative of tracking error  $e$  is  $\dot{e} = \dot{x} - \dot{x}_r$ . To obtain a fixed-time integral sliding mode controller, the error is reconstructed based on Lemma 3:

$$s = \dot{e} + k_1 [e]^\alpha + k_2 [e]^\beta \quad (14)$$

where  $k_1$ ,  $k_2$ ,  $\alpha$ ,  $\beta$  are all positive constants satisfying  $k_1, k_2 > 0$ ,  $0 < \alpha < 1$  and  $\beta > 1$ . When the sliding surface  $s$  converges to zero, (14) can be rewritten as:

$$\dot{e} = -k_1 [e]^\alpha - k_2 [e]^\beta \quad (15)$$

According to Lemma 3, the convergence time of (15) is bounded by:

$$T_{s1} \leq \frac{1}{k_1(1-\alpha)} + \frac{1}{k_2(\beta-1)} \quad (16)$$

Differentiating (14) with respect to time and using (5), we have:

$$\dot{s} = \ddot{x} - \ddot{x}_r + k_1 \alpha [e]^{\alpha-1} \dot{e} + k_2 \beta [e]^{\beta-1} \dot{e} = \Xi u + \Gamma(x, \dot{x}) + \Psi(x, \dot{x}, t) - \ddot{x}_r + k_1 \alpha [e]^{\alpha-1} \dot{e} + k_2 \beta [e]^{\beta-1} \dot{e} \quad (17)$$

Based on (14), the integral sliding surface is selected as:

$$\sigma_1(t) = s(t) - s(0) - \int_0^t (\Xi u_0 + \Gamma(x, \dot{x}) - \ddot{x}_r + k_1 \alpha [e]^{\alpha-1} \dot{e} + k_2 \beta [e]^{\beta-1} \dot{e}) dt \quad (18)$$

where term  $s(0)$  represents the value of the sliding surface when  $t = 0$ , which is added to eliminate the initial error.  $u_0$  is the output of the nominal controller, which is designed for the non-disturbance system by another method (e.g., PID, CTC, etc.) and will be presented in the Section 3.4. The derivative of the integral sliding surface can be further written as:

$$\dot{\sigma}_1(t) = (\Xi u + \Gamma(x, \dot{x}) + \Psi(x, \dot{x}, t) - \ddot{x}_r + k_1 \alpha [e]^{\alpha-1} \dot{e} + k_2 \beta [e]^{\beta-1} \dot{e}) - (\Xi u_0 + \Gamma(x, \dot{x}) - \ddot{x}_r + k_1 \alpha [e]^{\alpha-1} \dot{e} + k_2 \beta [e]^{\beta-1} \dot{e}) \quad (19)$$

Therefore, we have:

$$\dot{\sigma}_1(t) = \Xi (u - u_0) + \Psi(x, \dot{x}, t)$$

Letting  $u = u_0 + u_{s1}$ , where  $u_{s1}$  is designed to compensate for disturbances based on  $u_0$ , we obtain:

$$\dot{\sigma}_1(t) = \Xi u_{s1} + \Psi(x, \dot{x}, t) \quad (20)$$

From (20), the proposed compensating controller  $u_{s1}$  is designed as:

$$u_{s1} = \Xi^{-1} (-(\rho + \varepsilon) \text{sign}(\sigma_1) - k_3 [\sigma_1]^p - k_4 [\sigma_1]^q) \quad (21)$$

where the  $k_3, k_4 > 0$ ,  $0 < p < 1$  and  $q > 1$ . Inserting the compensating controller  $u_{s1}$  into (20), yields:

$$\dot{\sigma}_1(t) = \Psi(x, \dot{x}, t) - (\rho + \varepsilon) \text{sign}(\sigma_1) - k_3 [\sigma_1]^p - k_4 [\sigma_1]^q \quad (22)$$

and

$$\dot{\sigma}_{1_i}(t) = \Psi_i(x, \dot{x}, t) - (\rho + \varepsilon) \text{sign}(\sigma_{1_i}) - k_3 [\sigma_{1_i}]^p - k_4 [\sigma_{1_i}]^q \quad (23)$$

Consider a Lyapunov function candidate:

$$V_1 = \frac{1}{2} \sum_{i=1}^N \sigma_{1_i}^2 \quad (24)$$

Differentiating the Lyapunov function (24), we have:

$$\begin{aligned} \dot{V}_1 &= \sum_{i=1}^N \sigma_{1_i} \dot{\sigma}_{1_i} \\ &= \sum_{i=1}^N \sigma_{1_i} (\Psi_i(x, \dot{x}, t) - (\rho + \varepsilon) \text{sign}(\sigma_{1_i}) - k_3 [\sigma_{1_i}]^p - k_4 [\sigma_{1_i}]^q) \\ &= \sum_{i=1}^N \left( \sigma_{1_i} \Psi_i(x, \dot{x}, t) - (\rho + \varepsilon) |\sigma_{1_i}| - k_3 [\sigma_{1_i}]^{p+1} - k_4 [\sigma_{1_i}]^{q+1} \right) \end{aligned} \quad (25)$$

By using Assumption 1, we have:

$$\dot{V}_1 \leq \sum_{i=1}^N \left( -k_3 [\sigma_{1_i}]^{p+1} - k_4 [\sigma_{1_i}]^{q+1} \right) \quad (26)$$

By using Lemma 1 and Lemma 2, we have:

$$\begin{aligned} \dot{V}_1 &\leq -k_3 \sum_{i=1}^N |\sigma_{1_i}|^{p+1} - k_4 \sum_{i=1}^N |\sigma_{1_i}|^{q+1} \\ &\leq -k_3 \sum_{i=1}^N \left( |\sigma_{1_i}|^2 \right)^{\frac{p+1}{2}} - k_4 \sum_{i=1}^N \left( |\sigma_{1_i}|^2 \right)^{\frac{q+1}{2}} \\ &\leq -k_3 \left( \sum_{i=1}^N |\sigma_{1_i}|^2 \right)^{\frac{p+1}{2}} - k_4 N^{\frac{1-q}{2}} \left( \sum_{i=1}^N |\sigma_{1_i}|^2 \right)^{\frac{q+1}{2}} \\ &= -k_3 2^{\frac{p+1}{2}} (V_1)^{\frac{p+1}{2}} - k_4 2^{\frac{q+1}{2}} N^{\frac{1-q}{2}} (V_1)^{\frac{q+1}{2}} \end{aligned} \quad (27)$$

Based on the Lemma 3, the above system is fixed-time stable and the convergence time is upper bounded as:

$$T_{r1} \leq \frac{1}{2^{\frac{p+1}{2}} k_3 \left( 1 - \frac{p+1}{2} \right)} + \frac{1}{2^{\frac{q+1}{2}} k_4 N^{\frac{1-q}{2}} \left( \frac{q+1}{2} - 1 \right)} \quad (28)$$

**Theorem 1.** The system (5) with controller  $u_s$  is fixed-time stable and the settling time is bounded by:

$$T \leq T_{s1} + T_{r1} + T_n \quad (29)$$

where  $T_{s1}$  and  $T_{r1}$  represent the convergence time of the sliding variable  $s$  and the system (5) with  $u_{s1}$  as the controller, respectively.  $T_n$  represents the convergence time of the system (5) with  $u_0$  as the nominal controller, which will be determined in Section 3.4.

**Proof.** It is clear that the convergence time of the entire system is smaller than the sum of the convergence times of each component (i.e., the convergence times of the sliding surface, compensating controller and nominal controller). This completes the proof.

**Remark 1.** The value for  $\rho$  of the controller in (21) was selected based on **Assumption 1**. In practice, we can use experiments to determine the bounded value of the uncertainty  $\rho$ . Another method which can be applied to approximate the value of parameter of  $\rho$  is to use an adaptive technique; for example, we can use an adaptive second-order super-twisting method<sup>20</sup> to estimate the adaptive gain and eliminate the chattering at the same time.

**Remark 2.** The use of the ‘sign’ function in the controller (21) will generate a chattering. To eliminate the chattering, a boundary layer method or second-order super-twisting method can be employed<sup>20</sup>.

### 3.3 | Nonsingular Problem

From (17), when  $e = 0$  and  $\dot{e} \neq 0$  the term  $k_1 \alpha [e]^{\alpha-1} \dot{e}$  results in a singular problem. To avoid the singularity, the error can be reconstructed as:

$$s = e + \frac{1}{k_5^m} [\dot{e} + k_6 [e]^n]^{\frac{1}{m}} \quad (30)$$

where  $k_5, k_6, m, n$  are all positive constants satisfying  $k_5, k_6 > 0$ ,  $0 < m < 1$  and  $n > 1$ . When the sliding surface variable converges to zero, (30) is equal to (14). Therefore, according to the Lemma 3, the convergence time of (30) is bounded by:

$$T_{s2} \leq \frac{1}{k_5(1-m)} + \frac{1}{k_6(n-1)} \quad (31)$$

Differentiating (30) with respect to time, we have:

$$\dot{s} = \dot{e} + \frac{1}{mk_5^m} [\dot{e} + k_6 [e]^n]^{\frac{1}{m}-1} (\ddot{e} + k_6 n [e]^{n-1} \dot{e}) \quad (32)$$

The integral sliding surface is selected as:

$$\sigma_2(t) = s(t) - s(0) - \int_0^t \left( \dot{e} + \frac{1}{mk_5^m} [\dot{e} + k_6 [e]^n]^{\frac{1}{m}-1} (\ddot{e} + k_6 n [e]^{n-1} \dot{e}) \right) dt \quad (33)$$

According to the (5), we have:

$$\ddot{e} = \ddot{x} - \ddot{x}_r = \Xi u + \Gamma(x, \dot{x}) - \ddot{x}_r \quad (34)$$

Inserting (34) into (33) and letting:

$$T_1(e, \dot{e}) = \frac{1}{mk_5^m} [\dot{e} + k_6 [e]^n]^{\frac{1}{m}-1} \quad (35)$$

$$T_2(e) = k_6 n [e]^{n-1} \dot{e}$$

The derivative of integral sliding surface can be written as:

$$\dot{\sigma}_2(t) = (\dot{e} + T_1(e, \dot{e})) (\Xi u + \Gamma(x, \dot{x}) + \Psi(x, \dot{x}, t) - \ddot{x}_r + T_2(e)) - (\dot{e} + T_1(e, \dot{e})) (\Xi u_0 + \Gamma(x, \dot{x}) - \ddot{x}_r + T_2(e)) \quad (36)$$

Setting  $u = u_0 + u_{s2}$ , we have:

$$\dot{\sigma}_2(t) = T_1(e, \dot{e}) (\Xi u_{s2} + \Psi(x, \dot{x}, t)) \quad (37)$$

Again, the controller  $u_{s2}$  can be designed as:

$$u_{s2} = \Xi^{-1} (-(\rho + \varepsilon) \text{sign}(\sigma_2) - k_3 [\sigma_2]^p - k_4 [\sigma_2]^q) \quad (38)$$

Inserting the compensating controller into (37), we have:

$$\dot{\sigma}_2(t) = T_1(e, \dot{e}) (\Psi(x, \dot{x}, t) - (\rho + \varepsilon) \text{sign}(\sigma_2) - k_3 [\sigma_2]^p - k_4 [\sigma_2]^q) \quad (39)$$

Considering a Lyapunov function candidate:

$$V_2 = \frac{1}{2} \sum_{i=1}^N \sigma_{2_i}^2 \quad (40)$$

Differentiating the Lyapunov function (24), we have:

$$\begin{aligned} \dot{V}_2 &= \sum_{i=1}^N \sigma_{2_i} \dot{\sigma}_{2_i} \\ &= \sum_{i=1}^N \sigma_{2_i} T_1(e, \dot{e}) (\Psi_i(x, \dot{x}, t) - (\rho + \varepsilon) \text{sign}(\sigma_{2_i}) - k_3 [\sigma_{2_i}]^p - k_4 [\sigma_{2_i}]^q) \\ &= T_1(e, \dot{e}) \sum_{i=1}^N \left( \sigma_{2_i} \Psi_i(x, \dot{x}, t) - (\rho + \varepsilon) |\sigma_{2_i}| - k_3 [\sigma_{2_i}]^{p+1} - k_4 [\sigma_{2_i}]^{q+1} \right) \\ &\leq T_1(e, \dot{e}) \sum_{i=1}^N \left( -k_3 [\sigma_{2_i}]^{p+1} - k_4 [\sigma_{2_i}]^{q+1} \right) \\ &\leq T_1(e, \dot{e}) \left( -k_3 2^{\frac{p+1}{2}} (V_2)^{\frac{p+1}{2}} - k_4 2^{\frac{q+1}{2}} N^{\frac{1-q}{2}} (V_2)^{\frac{q+1}{2}} \right) \end{aligned} \quad (41)$$

**Theorem 2.** The system (5) with controller  $u_{s2}$  is fixed-time stable and its settling time is bounded by:

$$T \leq T_{s2} + T_{r2} + T_n + \epsilon(\tau) \quad (42)$$

where  $T_{s2}$  and  $T_{r2}$  represent the convergence time of sliding variable  $s$  and the system (5) with  $u_{s2}$  as the controller, respectively.  $T_n$  represent the convergence time of the system (5) with  $u_0$  as the nominal controller.

**Proof.** From (39), we can see the fixed-time stability depends both on the term  $\left(-k_3 2^{\frac{p+1}{2}} (V_2)^{\frac{p+1}{2}} - k_4 2^{\frac{q+1}{2}} N^{\frac{1-q}{2}} (V_2)^{\frac{q+1}{2}}\right)$  and the term  $T_1(e, \dot{e})$ . According to the work of Van and Ceglarek<sup>20</sup>, for the case of  $\dot{e} + k_6 [e]^n \neq 0$ , we divide the state space into two different areas  $\Omega_1 = \{(e, \dot{e}) | T(e, \dot{e}) \geq 1\}$  and  $\Omega_2 = \{(e, \dot{e}) | T(e, \dot{e}) < 1\}$ .

i. When the system states are in the area of  $\Omega_1$ , we have:

$$\dot{V}_2 \leq -k_3 2^{\frac{p+1}{2}} (V_2)^{\frac{p+1}{2}} - k_4 2^{\frac{q+1}{2}} N^{\frac{1-q}{2}} (V_2)^{\frac{q+1}{2}} \quad (43)$$

$V_2 = 0$  implies the sliding surface  $s = 0$ . Therefore, according to the Lemma 3, the system states will reach the sliding surface  $s = 0$  within a fixed time, which is upper bounded as:

$$T_{r2} \leq \frac{1}{2^{\frac{p+1}{2}} k_3 \left(1 - \frac{p+1}{2}\right)} + \frac{1}{2^{\frac{q+1}{2}} k_4 N^{\frac{1-q}{2}} \left(\frac{q+1}{2} - 1\right)} \quad (44)$$

ii. When the system states are in the area of  $\Omega_2$ , according to (41), the sliding surface  $s = 0$  is still an attractor. In addition, for the case of  $\dot{e} + k_6 [e]^n = 0$ , for a given  $\tau$ , there exists a positive constant  $\epsilon(\tau)$  such that the sliding surface  $s_2 = 0$  can be reached from anywhere in the phase plane within a fixed time  $t_r < T_{r2} + \epsilon(\tau)$ .<sup>21</sup> Therefore, the total setting time  $T$  is bounded as (42). This completes the proof.

**Remark 3.** Compared to the design of the integral sliding surfaces of the existing FTISM<sup>11,12,13</sup>, the proposed controller uses the sliding surface in (33), which takes the dynamics of the system account in the design of the integral sliding surface. This approach provides two advantages: (1) it allows us to design the nominal controller  $u_0$  and the reaching controller  $u_s$  separately. This facilitates the design procedure and preserves the advantages of both the nominal controller and ISMC.

### 3.4 | Design of the Nominal Controller

The nominal controller is designed to stabilize the system neglecting the lumped uncertainties. To stabilize the whole system within a fixed time, we choose fixed-time backstepping control<sup>22</sup> as the nominal controller. The dynamics of the robot manipulator without lumped uncertainties can be written as:

$$\begin{cases} \dot{\eta}_1 = \eta_2 \\ \dot{\eta}_2 = \Xi u + \Gamma(x, \dot{x}) \end{cases} \quad (45)$$

Letting  $s_1 = \eta_1 - x_r$ , then,  $\dot{s}_1 = \eta_2 - \dot{x}_r$ , and we can design the stabilizing function as:

$$\alpha_s = -\left(\lambda_1 s_1 + \lambda_2 s_1^\alpha + \lambda_3 s_1^\beta\right) + \dot{x}_r \quad (46)$$

where  $\lambda_1, \lambda_2, \lambda_3, \alpha, \beta$  are all positive constants satisfying  $0 < \alpha < 1$  and  $\beta > 1$ . Thus,  $\dot{s}_1$  can be written as:

$$\dot{s}_1 = -\left(\lambda_1 s_1 + \lambda_2 s_1^\alpha + \lambda_3 s_1^\beta\right) \quad (47)$$

Selecting the Lyapunov function candidate as:

$$V_3 = \frac{1}{2} s_1^T s_1 \quad (48)$$

The derivative of the Lyapunov function  $V_3$  is:

$$\begin{aligned}
\dot{V}_3 &= s_1^T \dot{s}_1 \\
&= -s_1^T \left( \lambda_1 s_1 + \lambda_2 s_1^\alpha + \lambda_3 s_1^\beta \right) \\
&= -\lambda_1 s_1^T s_1 - \lambda_2 \left( s_1^T s_1 \right)^{\frac{\alpha+1}{2}} - \lambda_3 \left( s_1^T s_1 \right)^{\frac{\beta+1}{2}} \\
&\leq -\lambda_2 \left( s_1^T s_1 \right)^{\frac{\alpha+1}{2}} - \lambda_3 \left( s_1^T s_1 \right)^{\frac{\beta+1}{2}} \\
&\leq -2^{\frac{\alpha+1}{2}} \lambda_2 \left( \frac{1}{2} s_1^T s_1 \right)^{\frac{\alpha+1}{2}} - 2^{\frac{\beta+1}{2}} \lambda_3 \left( \frac{1}{2} s_1^T s_1 \right)^{\frac{\beta+1}{2}} \\
&= -2^{\frac{\alpha+1}{2}} \lambda_2 (V_3)^{\frac{\alpha+1}{2}} - 2^{\frac{\beta+1}{2}} \lambda_3 (V_3)^{\frac{\beta+1}{2}}
\end{aligned} \tag{49}$$

Letting  $s_2 = \eta_2 - \alpha_s$ , we have:

$$\dot{s}_2 = \dot{\eta}_2 - \dot{\alpha}_s = \Xi u_0 - \Gamma(x, \dot{x}) - \dot{\alpha}_s \tag{50}$$

Selecting the Lyapunov function candidate as:

$$V_4 = \frac{1}{2} s_2^T s_2 \tag{51}$$

To obtain the property of fixed-time convergence, we design the nominal controller as:

$$u_0 = \Xi^{-1} \left( -\Gamma(x, \dot{x}) + \dot{\alpha}_s - \lambda_1 s_2 - \lambda_2 s_2^\alpha - \lambda_3 s_2^\beta \right) \tag{52}$$

Inserting (52) into (50), we have:

$$\dot{s}_2 = -\lambda_1 s_2 - \lambda_2 s_2^\alpha - \lambda_3 s_2^\beta \tag{53}$$

The derivative of the Lyapunov function  $V_2$  is:

$$\begin{aligned}
\dot{V}_4 &= s_2^T \dot{s}_2 \\
&= s_2^T \left( -\lambda_1 s_2 - \lambda_2 s_2^\alpha - \lambda_3 s_2^\beta \right) \\
&\leq -2^{\frac{\alpha+1}{2}} \lambda_2 (V_4)^{\frac{\alpha+1}{2}} - 2^{\frac{\beta+1}{2}} \lambda_3 (V_4)^{\frac{\beta+1}{2}}
\end{aligned} \tag{54}$$

Choosing the Lyapunov function candidate of system as:

$$V_n = V_3 + V_4 \tag{55}$$

The derivative of Lyapunov function  $V$  is:

$$\begin{aligned}
\dot{V}_n &\leq -2^{\frac{\alpha+1}{2}} \lambda_2 (V_3)^{\frac{\alpha+1}{2}} - 2^{\frac{\beta+1}{2}} \lambda_3 (V_3)^{\frac{\beta+1}{2}} - 2^{\frac{\alpha+1}{2}} \lambda_2 (V_4)^{\frac{\alpha+1}{2}} - 2^{\frac{\beta+1}{2}} \lambda_3 (V_4)^{\frac{\beta+1}{2}} \\
&\leq -2^{\frac{\alpha+1}{2}} \lambda_2 (V_n)^{\frac{\alpha+1}{2}} - 2^{\frac{\beta+1}{2}} \lambda_3 (V_n)^{\frac{\beta+1}{2}}
\end{aligned} \tag{56}$$

According to the Lemma 3, when applying the proposed nominal controller  $u_0$ , the system without lumped uncertainties is fixed-time stable and the convergence time is bounded as:

$$T_n \leq \frac{2}{\lambda_2 2^{\frac{\alpha+1}{2}} (1 - \alpha)} + \frac{2}{\lambda_3 2^{\frac{\beta+1}{2}} (\beta - 1)} \tag{57}$$

*Remark 4.* It is noted that the nominal controller can be designed using other controllers, e.g, PID, CTC and Backstepping. However, in this paper, we use the fixed-time backstepping controller to achieve global fixed-time convergence for the system.

## 4 | SIMULATION AND RESULTS

In the simulation, we consider a two-link robot in the horizontal plane<sup>23</sup>. The dynamics of the robot are described as:

$$\begin{aligned}
\tau_1 &= m_2 l_2^2 (\ddot{q}_1 + \ddot{q}_2) + m_2 l_1 l_2 c_2 (2\dot{q}_1 + \dot{q}_2) + (m_1 + m_2) l_1^2 \ddot{q}_1 - m_2 l_1 l_2 s_2 \dot{q}_2^2 - 2m_2 l_1 l_2 s_2 \dot{q}_1 \dot{q}_2 + m_2 l_2 g c_{12} + (m_1 + m_2) l_1 g c_1 \\
\tau_2 &= m_2 l_1 l_2 c_2 \dot{q}_1 + m_2 l_1 l_2 s_2 \dot{q}_1^2 + m_2 l_2 g c_{12} + m_2 l_2^2 (\ddot{q}_1 + \ddot{q}_2)
\end{aligned} \tag{58}$$

where  $c_i = \cos(q_i)$ ,  $c_{ij} = \cos(q_i + q_j)$ ,  $s_i = \sin(q_i)$ , and  $s_{ij} = \sin(q_i + q_j)$ ,  $i, j = 1, 2$ . The value of masses are  $m_1 = 1.5kg$ , and  $m_2 = 1.0kg$ . The length of the links are  $l_1 = l_2 = 0.3m$ . Based on the (1), the mass matrix  $M(q)$ , Coriolis and centrifugal forces matrix  $C(q, \dot{q})$  and the gravity matrix  $G(q)$  are given as:

$$M(q) = \begin{bmatrix} m_2 l_2^2 + 2m_2 l_1 l_2 c_2 + (m_1 + m_2) l_1^2 & m_2 l_2^2 + m_2 l_1 l_2 c_2 \\ m_2 l_2^2 + m_2 l_1 l_2 c_2 & m_2 l_2^2 \end{bmatrix} \quad (59)$$

$$C(q, \dot{q}) = \begin{bmatrix} -2m_2 l_1 l_2 s_2 \dot{q}_2 & -m_2 l_1 l_2 s_2 \\ m_2 l_1 l_2 s_2 \dot{q}_1 & 0 \end{bmatrix} \quad (60)$$

$$G(q) = \begin{bmatrix} m_2 l_2 g c_{12} + (m_1 + m_2) l_1 g c_1 \\ m_2 l_2 g c_{12} \end{bmatrix} \quad (61)$$

The bounded disturbance term is given as:

$$F(q) = \begin{bmatrix} 2c_1 s_2 + 5c_1^2 \\ -2c_1 s_2 - 5c_1^2 \end{bmatrix} \quad (62)$$

The Jacobian of the robot manipulator is given as:

$$J(q) = \begin{bmatrix} -l_1 s_1 - l_2 s_{12} & -l_2 s_{12} \\ l_1 c_1 + l_2 c_{12} & l_2 c_{12} \end{bmatrix} \quad (63)$$

Assume the desired trajectory<sup>3</sup> of the two joints is:

$$\begin{aligned} x_{d1}(t) &= 0.14 \cos(0.5t) \\ x_{d2}(t) &= 0.14 \sin(0.5t) \end{aligned} \quad (64)$$

The external human forces, as shown in Fig. 5, are given by<sup>3</sup>:

$$f e_i(t) \begin{cases} 0 & t < 10 \text{ or } t \geq 21 \\ a_i (1 - \cos \pi t) & 10 \leq t < 11 \\ 2a_i & 11 \leq t < 20 \\ a_i (1 + \cos \pi t) & 20 \leq t < 21 \end{cases} \quad (65)$$

The external human forces are applied when  $t = 10s$  and removed at  $t = 21s$ . By applying admittance control, the reference trajectory of the two joints  $x_{r1}$  and  $x_{r2}$  can be derived by integrating equation (12) twice. Fig. 4 shows both the desired trajectory and the reference trajectory. We can see the two trajectories are the same before the external forces are applied. When  $t > 10s$ , the reference trajectory, which complies with the external human forces, is different from the desired trajectory. When  $t > 21s$ , the external human forces are removed from the contact point and the two trajectories coincide again.

To verify the effectiveness of the proposed controller, we compare it with PID, computed torque control (CTC), traditional ISMC with PID as the nominal controller (ISMC PID), traditional ISMC with CTC as the nominal controller (ISMC CTC), and traditional ISMC with BSP as the nominal controller (ISMC BSP). Assume the initial position of the end-effector is  $q(0) = [0.5236, 2.0944]^T$ , and the initial value of the task variable is  $x(0) = [0, 0]^T$ . The design parameters of the admittance control are  $k_{m_i} = 20$ ,  $k_{b_i} = 20$  and  $k_{k_i} = 100$ ,  $i = 1, 2$ . The PID parameters are  $k_p = 300$ ,  $k_d = 400$ ,  $k_i = 10$ . The parameters of BSP are

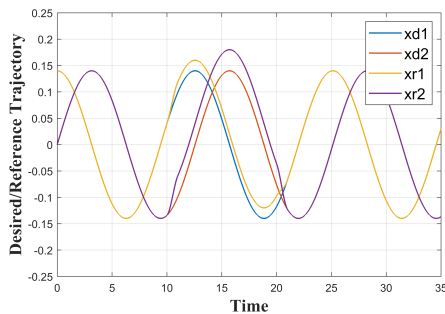


FIGURE 4 Desired/reference trajectory.

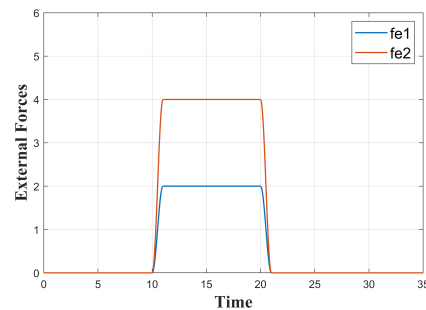


FIGURE 5 External human forces.

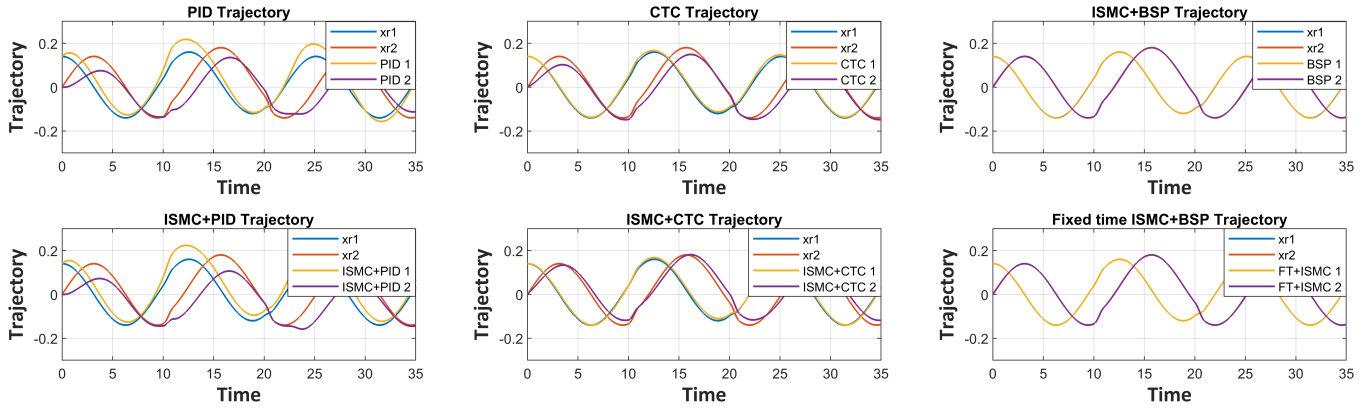


FIGURE 6 Trajectories obtained with the different controllers.

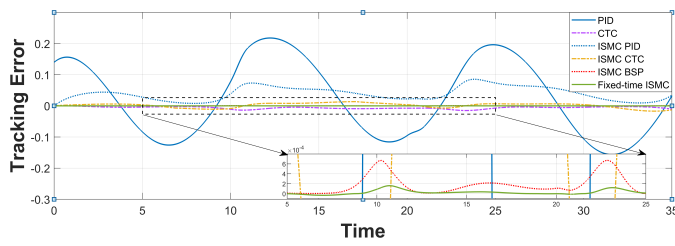


FIGURE 7 Tracking error for joint 1.

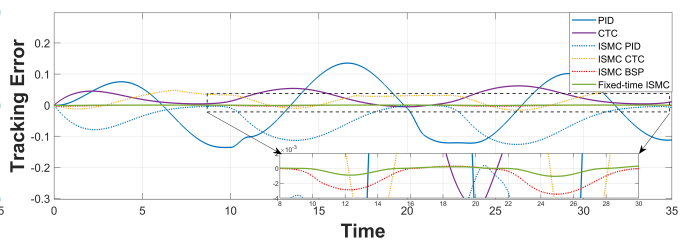


FIGURE 8 Tracking error for joint 2.

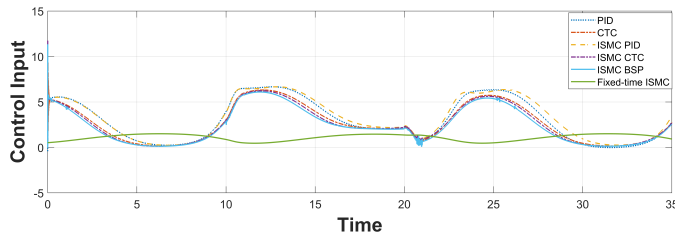


FIGURE 9 Control input for joint 1.

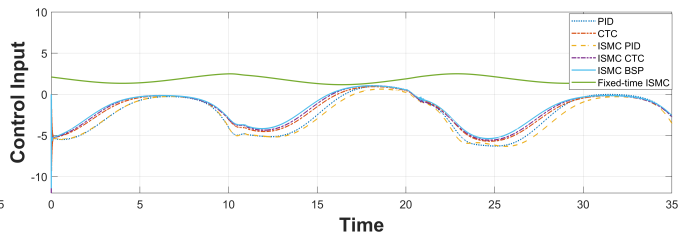


FIGURE 10 Control input for joint 2.

$\lambda_1 = 3, \lambda_2 = 20, \lambda_3 = 50, \alpha = \frac{5}{7}, \beta = \frac{5}{3}$ . These parameters are selected based on a trial-and-error procedure and by experience. The design parameters of the proposed controller are  $k_1 = k_3 = 20, k_2 = k_4 = 50, m = p = \frac{5}{7}, n = q = \frac{5}{3}$ .

The trajectories of the benchmark controllers and the proposed fixed-time ISMC controller with BSP as the nominal controller are shown in Fig. 6, and the corresponding Root Mean Square Error (RMSE) of tracking errors are reported in Table 1. We can see that the PID controller has the poorest tracking performance. The performances of CTC is a little better than PID. The performance of ISMC PID and ISMC CTC are better than pure PID and CTC, respectively, which means the tracking performance of the controller is improved by adding the integral sliding surface. The ISMC BSP and proposed fixed-time ISMC controller have the best tracking performance. They almost achieve perfectly tracking of the reference trajectory, which makes it difficult to compare them in Fig. 6. However, as can be seen in Fig. 7 and Fig. 8, it is clear that the proposed controller has both the smallest tracking error and shortest convergence time. Note that the proposed controller is global fixed-time convergent because both the integral sliding surface, reaching controller and the nominal controller can converge within a fixed time. In addition, from Fig. 9 and Fig. 10, which show the control inputs of the two joints, it can be seen that the proposed solution provides the smoothest and most efficient control input.

**TABLE 1** The RMSE performance of each controller.

Joint	PID	CTC	ISMC+PID	ISMC+CTC	ISMC+BSP	FTISMC+BSP
1	0.1211	0.0070	0.0446	0.0064	$2.0901 \times 10^{-4}$	$5.7841 \times 10^{-5}$
2	0.0845	0.0314	0.0644	0.0220	0.0016	$4.4889 \times 10^{-4}$

## 5 | CONCLUSIONS

In this paper, a fixed-time ISMC controller based on admittance control has been proposed for robot manipulators such that the robot can comply with the external human forces rather than reject them as disturbances. Furthermore, the convergence time of the system can be predefined regardless of the initial conditions. The simulation results show that the proposed controller can track the reference trajectory precisely with faster convergence of the tracking error. In future work, a fixed-time force observer of external human forces will be discussed and integrated into the system. Safety constraints of the system will also be considered. The whole system will be tested on a robotics platform such as the Baxter robot to further validate the controller's effectiveness and evaluate real world performance.

## References

1. Sharifi M, Azimi V, Mushahwar VK, Tavakoli M. Impedance Learning-Based Adaptive Control for Human-Robot Interaction. *IEEE Transactions on Control Systems Technology* 2021; 1-14.
2. He W, Xue C, Yu X, Li Z, Yang C. Admittance-based controller design for physical human-robot interaction in the constrained task space. *IEEE Transactions on Automation Science and Engineering* 2020; 17(4): 1937-1949.
3. Tee KP, Yan R, Li H. Adaptive admittance control of a robot manipulator under task space constraint. In: IEEE. ; 2010: 5181-5186.
4. Okunev V, Nierhoff T, Hirche S. Human-preference-based control design: Adaptive robot admittance control for physical human-robot interaction. In: IEEE. ; 2012: 443-448.
5. Huang L. An adaptive impedance control scheme for constrained robots. 2004.
6. Tsumugiwa T, Yokogawa R, Hara K. Variable impedance control based on estimation of human arm stiffness for human-robot cooperative calligraphic task. In: . 1. IEEE. ; 2002: 644-650.
7. Chan S, Yao B, Gao W, Cheng M. Robust impedance control of robot manipulators.. *International Journal of Robotics & Automation* 1991; 6(4): 220-227.
8. Liu G, Goldenberg AA. Robust hybrid impedance control of robot manipulators. In: IEEE Computer Society. ; 1991: 287-288.
9. Zuo Z. Non-singular fixed-time terminal sliding mode control of non-linear systems. *IET control theory & applications* 2015; 9(4): 545-552.
10. Van M. Adaptive neural integral sliding-mode control for tracking control of fully actuated uncertain surface vessels. *International Journal of Robust and Nonlinear Control* 2019; 29(5): 1537-1557.
11. Huang S, Wang J. Robust fixed-time integral sliding mode control of a nonlinear hydraulic turbine regulating system. *Journal of Computational and Nonlinear Dynamics* 2020; 15(3): 031002.
12. Li B, Zhang H, Xiao B, Wang C, Yang Y. Fixed-time integral sliding mode control of a high-order nonlinear system. *Nonlinear Dynamics* 2021.

13. Wang JB, Liu CX, Wang Y, Zheng GC. Fixed time integral sliding mode controller and its application to the suppression of chaotic oscillation in power system. *Chinese Physics B* 2018; 27(7): 070503.
14. Shi S, Gu J, Xu S, Min H. Globally Fixed-Time High-Order Sliding Mode Control for New Sliding Mode Systems Subject to Mismatched Terms and Its Application. *IEEE Transactions on Industrial Electronics* 2020; 67(12): 10776-10786.
15. Yang C, Jiang Y, He W, Na J, Li Z, Xu B. Adaptive parameter estimation and control design for robot manipulators with finite-time convergence. *IEEE Transactions on Industrial Electronics* 2018; 65(10): 8112–8123.
16. Zuo Z, Tie L. Distributed robust finite-time nonlinear consensus protocols for multi-agent systems. *International Journal of Systems Science* 2016; 47(6): 1366–1375.
17. Feng Y, Yu X, Man Z. Non-singular terminal sliding mode control of rigid manipulators. *Automatica* 2002; 38(12): 2159–2167.
18. Yang L, Yang J. Nonsingular fast terminal sliding-mode control for nonlinear dynamical systems. *International Journal of Robust and Nonlinear Control* 2011; 21(16): 1865–1879.
19. Zuo Z. Nonsingular fixed-time consensus tracking for second-order multi-agent networks. *Automatica* 2015; 54: 305–309.
20. Van M, Ceglarek D. Robust fault tolerant control of robot manipulators with global fixed-time convergence. *Journal of the Franklin Institute* 2021; 358(1): 699–722.
21. Li H, Cai Y. On SFTSM control with fixed-time convergence. *Int Control Theory and Applications* 2017; 11: 766-773.
22. Van M, Sun Y, McIlvanna S, Khyam M, Ceglarek D. Adaptive fuzzy fault tolerant control for robot manipulators with fixed-Time convergence. In: .
23. Craig JJ, Hsu P, Sastry SS. Adaptive control of mechanical manipulators. *The International Journal of Robotics Research* 1987; 6(2): 16–28.

**How to cite this article:** Sun Y., Van M., McIlvanna S., McLoone S., and Ceglarek D. (2022), Fixed-time Integral Sliding Mode Control for Admittance Control of a Robot Manipulator, *Manuscript submitted for publication*..